Combinatorial Investigation of Structural Quality of Au/Ni Contacts on GaN

A.V. Davydov [a*], L.A. Bendersky [a], W.J. Boettinger [a], D. Josell [a], M.D. Vaudin [b], K.-S. Chang [c] and I. Takeuchi [c]

[a] Metallurgy Division / [b] Ceramic Division, NIST, Gaithersburg, MD
[c] Dept. of Materials and Nuclear Engineering, University of Maryland, College Park, MD

Abstract

A combinatorial library of Au/Ni metallizations on GaN was microstructurally characterized by x-ray diffraction (XRD), electron back-scattered diffraction (EBSD) and transmission electron microscopy (TEM). The array of single- and bi-layered metal elements of systematically varying thicknesses was deposited by electron-beam evaporation on a GaN/c-sapphire wafer. The elements with a single layer of Au on GaN had a fiber texture with <111> preferred growth orientation. TEM revealed a 2 nm thick amorphous contamination layer between the Au and GaN, which prevented the gold from being epitaxial. By contrast, nickel in both the single-layered Ni and bi-layered Au/Ni elements formed epitaxially on the GaN with a $(111)_{fcc}//(0001)_{hex}$, $<110>_{fcc}//<11\bar{2}0>_{hex}$ orientation relation, as observed by TEM and EBSD. The Ni layer formed two types of domains related by a 60° rotation about $<111>_{fcc}$, which were replicated by the Au over-layer in the Au/Ni structures. The improved structural quality of the bi-layered Au/Ni as compared to the single-layered Au was due to the removal of native contamination from the GaN surface during the initial step of Ni deposition; this promoted epitaxial growth of both metal layers. However, as the nickel inter-layer thickness was increased above 5 nm, the Au/Ni structural quality decreased, as measured by increased deviations from the $(111)_{fcc}//(0001)_{hex}$ orientation relation.

PACS: 68.55.J, 68.65, 73.40.N
Keywords: GaN, metal contacts, combinatorial material science, thin films

Introduction

The performance of GaN-based optoelectronic and electronic devices is limited by several materials and engineering problems, including the difficulty of making reliable metal contacts [1]. The reliability issues include the requirements for contacts to be microstructurally, electrically and optically uniform and thermally stable. Bi-layered Au/Ni metallization is commonly used for both Ohmic contacts to p-type GaN [2] and Schottky contacts to n-GaN [3]. Metal contact non-uniformity and thermal instability, often manifested in Au/Ni intermixing and interfacial reactions with the GaN even at room temperature [4,5], is thought to be promoted by fast diffusion at the

grain boundaries in the metal layers. For this reason, it is advantageous for metal contacts to be epitaxial on the GaN. Indeed, epitaxial Au/Ni-based contacts have been noted to provide uniform electrical characteristics, enhanced thermal stability and high optical transparency [6-10]. It has been reported that Au or Ni epitaxy is attained by depositing metals on atomically clean gallium nitride surface, where the surface contamination layer (hereafter called "SCL") is removed. It was found that the SCL consists of a mixture of amorphous gallium oxides/oxynitrides [11,12] and can be completely removed in vacuum or in various ambients at elevated temperatures [9,13,14]. On the other hand, Ni and Au deposited on wet-etched GaN surface are typically polycrystalline [5,15-18] with Au contacts additionally suffering from adhesion problems [15,19]. Poor structural and adhesive qualities of metals in the latter case are likely caused by the presence of the SCL on the GaN surface, which often remains or re-forms after standard acid/base wet cleaning of the GaN surface [8,20,21].

The structural quality of the metal contacts, as well as their optical and electrical properties [22,23], are also affected by the Au/Ni ratio and the layer thicknesses. Therefore, it is important to determine the range of optimum Au/Ni ratios and thicknesses for the best crystal quality of metal contacts. Since optimization of the metallization scheme requires extensive experimentation, the methods of high-throughput (combinatorial) experimental research are ideal for this task. This paper presents the results of a combinatorial study, in which the crystal quality of as-deposited Au/Ni contacts to GaN is correlated with the metal bi-layer ratio and thickness variations. In a separate paper of this journal issue, results of spectroscopic reflectometry and transmission of as-deposited and heat-treated contacts as a function of Au/Ni ratio and thickness are reported [24].

Experimental

The GaN used for the Au/Ni contact study was obtained commercially from Technologies and Devices International, Inc[*]. A 5 μm thick GaN epilayer was grown by hydride-vapor-phase epitaxy on a 2" sapphire (0001) substrate. The GaN was Si-doped n-type with a bulk carrier concentration of 10^{18} cm^{-3}. Prior to metallization, the GaN surface was degreased sequentially in boiling chloroform, acetone, and iso-propanol solutions. After degreasing, the GaN surface was etched in a cold HF:H_2O (1:1) mixture for 2 min, rinsed in de-ionized (DI) water, and etched again in a boiling NH_4OH:H_2O_2:H_2O (1:1:3) mixture for 10 min. Etching was followed by washing in boiling DI water and iso-propanol. After this wet-etch cleaning process, the sample was blown dry with

[*] Corresponding author. Tel. +1-301-975-4916; fax: +1-301-975-4916 E-mail address: davydov@nist.gov
[*] Certain commercial equipment, instruments, or materials supplier are identified in this paper in order to specify the experimental procedure adequately and do not imply endorsement by NIST

nitrogen gas and immediately loaded into the vacuum system for metal deposition by electron-beam evaporation. Ni and Au were deposited sequentially at 0.5 nm/s onto the GaN, which was held at room temperature. The base pressure of the chamber prior to deposition was 3×10^{-8} Torr; the pressure during deposition did not exceed 8×10^{-8} Torr. A shutter system was used to create a library array of ninety-one 5 mm square elements, each with either single-layered Au/GaN or bi-layered Au/Ni/GaN elements with the thicknesses indicated in **Fig. 1**. A sub-set of individual Au/Ni/GaN 12x6 mm samples, duplicating selected combinatorial elements, was prepared separately for destructive transmission electron microscopy (TEM) cross section analysis.

The crystalline quality of the Au/Ni/GaN library was assessed by x-ray diffraction (XRD) and electron back-scattered diffraction (EBSD). The XRD scans were collected on a Bruker-AXS D8 scanning x-ray micro-diffractometer equipped with a general area detector diffraction system (GADDS) using Cu Kα radiation. The two dimensional $2\theta - \chi$ GADDS patterns were collected in the 32^o to 52^o 2θ range. The metal/GaN interfaces in selected Au/GaN and Au/Ni/GaN samples were also studied using low- and high-resolution TEM cross-section analysis.

Results and Discussion

The EBSD, XRD, and TEM analyses revealed differences in the structural quality of the Au/GaN vs. the Au/Ni/GaN elements. The typical XRD GADDS spectrum of the Au/GaN sample in **Fig. 2a** shows that the gold deposited directly on the gallium nitride has a fiber texture with the <111> preferred orientation along the normal to the GaN basal plane. Analysis of the Au 111 profile along the χ direction showed that approximately 90% of the grains had up to 7^o misorientation between the $<111>_{Au}$ and the $<0001>_{GaN}$. The cross-section TEM of the Au(35nm)/GaN sample confirmed the <111> fiber texture in the Au layer with significant deviations of $<111>_{Au}$ away from $<0001>_{GaN}$ (**Fig. 3a**). The EBSD produced no diffraction pattern from any of the Au/GaN library elements, which is consistent with the fine Au grain size and a spread of the $<111>_{Au}$ orientations as observed in the XRD and TEM.

Unlike the Au/GaN case, the single-layered Ni and the bi-layered Au/Ni library elements produced less extended (more spot-like) 111 reflections in the XRD GADDS spectra (**Fig. 2b** and **c**) and well-defined EBSD diffraction patterns, although of different sharpnesses (**Fig. 4a** and **b**). The EBSD diffraction patterns from the Ni, Au and GaN were well aligned throughout the wafer, a fact which confirms that the Ni layer is epitaxial with the GaN and that the Au layer, in turn, is epitaxial with the Ni layer. The fact that the diffraction images appeared to be motionless while the

electron beam was translated over the library elements, indicates little (less than 0.1º) tilt of the $<111>_{fcc}$ from the $<0001>_{hex}$ orientation, as well as no rotational, i.e. relative to the $(0001)_{hex}$ plane, type of misorientation in both the Ni and Au.

To understand the difference in crystal quality of the gold layers with and without the Ni under-layer, cross-section high-resolution TEM images of Au/GaN (**Fig. 3a**) and Au/Ni/GaN (**Fig. 3b**) were analyzed. For the Au/GaN case, HRTEM revealed the presence of a 2 nm thick amorphous layer between the Au and the GaN. This is likely to be a native oxynitride-based SCL that resides on the GaN surface. This evidence of residual GaN surface contamination after standard wet cleaning procedure is consistent with previous TEM observations [13]. Evidently, the amorphous SCL prevented the gold from growing epitaxially on the GaN. In contrast, the Ni/GaN interface in **Fig. 3b** was abrupt and clean with the Ni layer epitaxial on the GaN. Apparently, the SCL was completely removed from the GaN surface through reaction with the nickel during the metal deposition. Previous reports found that as-deposited nickel significantly reduces the thickness of the GaN contamination layer [25] but that additional annealing of Ni/GaN structures is required to remove it completely from the GaN surface [13]. One explanation for the efficiency of nickel in dispersing the oxynitride-based contamination layer is the several orders of magnitude higher solubility of oxygen and nitrogen in nickel compared to that in gold [26].

Even though the nickel under-layer promotes gold epitaxy, it is important to note that the structural quality of the Au over-layer decreased as the Ni layer thickness was increased. For example, in a comparison of EBSD patterns from 35 nm thick Au deposited on 5 nm Ni (**Fig. 4a**) and on 65 nm Ni (**Fig. 4b**), a clear loss of contrast is evident in the latter pattern. Likewise, comparing the XRD GADDS images for the Au(35nm)/Ni(5 to 65 nm) elements in **Figs. 2b-d** shows that the 111 reflections for both Ni and Au systematically elongate in the χ direction as the Ni thickness increases. Analysis of the full width at half maximum (FWHM) of the χ profiles for 111_{Au} and 111_{Ni} confirmed this observation. For the 5 nm, 15 nm and 65 nm Ni interlayer, the FWHM for the 111_{Au} χ profile was 0.9°, 1.8° and 3.2° respectively. At each Ni layer thickness, the 111 χ FWHM values for Au and Ni are similar, showing that the degree of orientation of the Ni layer is duplicated in the Au deposited on it. Thus, with increasing thickness of the Ni inter-layer, increasing deviation from the $(111)_{fcc}//(0001)_{hex}$ orientation relation in the Ni-on-GaN layer is seen and it is replicated in the gold over-layer. This increasing misorientation of the Ni layer with thickness may be induced by relaxation of the substantial 22% mismatch between the $(111)_{Ni}$ and $(0001)_{GaN}$ planes, and it requires further investigation.

Two other noteworthy morphological features were observed in the Au/Ni bi-layers. First, TEM revealed that the Au grains were typically an order of magnitude larger than the Ni grains

(see **Fig. 3c**). Second, two types of crystalline domains were observed in the nickel layer (**Fig. 3b**) that were also mimicked in the gold over-layer in the Au/Ni structures (**Fig. 4a**). According to the TEM and EBSD results, the domains of type I and type II were in a twin relationship, with a 60° rotation about $<111>_{fcc}$, and were aligned with the GaN lattice as follows: $(111)_{I,II}//(0001)_{GaN}$ (common for both domains); $[1\,\bar{1}\,0]_I//[11\,\bar{2}\,0]_{GaN}$ and $[1\,\bar{1}\,0]_{II}//[\bar{1}\,2\,\bar{1}\,0]_{GaN}$, respectively. Formation of two types of domains in the Ni layer adjacent to the GaN can be explained by the two different ways of stacking close-packed $\{111\}_{fcc}$ planes on the $(0001)_{hex}$ plane: e.g. ABCA... (type I) and ACBA... (type II).

Conclusions

The structural quality of the Au and Ni single- and bi-layered combinatorial library on a GaN/sapphire substrate was investigated as a function of the metal ratios and thicknesses using XRD, EBSD and TEM. For the best structural quality, it was found advantageous to first deposit a thin layer of nickel onto GaN. Nickel appeared to dissolve the native contamination layer from the GaN surface during deposition, which promoted epitaxial growth of the gold over-layer. By contrast, a direct deposition of gold on GaN resulted in the formation of non-epitaxial, fiber-textured layer with significant grain misorientation due to the presence of the amorphous contamination layer on the GaN surface. However, an increased Ni inter-layer thickness in the Au/Ni structures had an adverse effect on their structural quality due to increased deviations from the $(111)_{fcc}//(0001)_{hex}$ orientation relation in the Ni-on-GaN layer, replicated in the Au over-layer. Thus, the best structural quality of the Au/Ni layers in the combinatorial library was obtained with the thinnest (5 nm) nickel inter-layer.

Acknowledgements

The authors wish to acknowledge R.L. Parke from NIST for the TEM sample preparation.

References

[1] Q.Z. Liu, S.S. Lau, Solid-State Electronics, 42 (1998) 677
[2] S. Nakamura, M. Senoh, S. Nagahama, N. Iwasa, T. Yamada, T. Matsushita, H. Kiyoku, Y. Sugimoto, Jap. J. Appl. Phys., 35 (1996) L74
[3] B. J. Zhang, T. Egawa, G. Y. Zhao, H. Ishikawa, M. Umeno, and T. Jimbo, Appl. Phys. Lett., 79 (2001) 2567
[4] V.M. Bermudez, R. Kaplan, M.A. Khan, and J.N. Kuznia, Phys. Rev. B, 48 (1993) 2436
[5] E. Kaminska, A. Piotrowska, J. Jasinski, J. Kozubowski, A. Barcz, K. Golaszewska, D.B. Thomson, R.F. Davis, M.D. Bremser, MRS Internet J. Nitride Semicond. Res., 4S1 (1999) G9.9
[6] Q.Z. Liu, S.S. Lau, N.R. Perkins, and T.F. Kuech, Appl. Phys. Lett., 69 (1996) 1722
[7] J.-S. Jang, S.-J. Park, and T.-Y. Seong, J. Appl. Phys., 88 (2000) 5490
[8] P.J. Hartlieb, A. Roskowski, R.J. Nemanich, and R.F. Davis, J. Appl. Phys., 91 (2002) 9151
[9] E.A. Preble, K.M. Tracy, S. Kiesel, H. McLean, P.Q. Miraglia, R.J. Nemanich, M. Albrecht,

D.J. Smith, and R.F. Davis, J. Appl. Phys., 91 (2002) 2133
[10] J. Narayan, H. Wang, T.-H. Oh, H.K. Choi, and J.C.C. Fan, Appl. Phys. Lett., 81 (2002) 3978
[11] K. Prabhakaran, T.G. Anderson, and K. Nozawa, Appl. Phys. Lett., 69 (1996) 3212
[12] P. J. Hartlieb, A. Roskowski, R. F. Davis, W. Platow, and R. J. Nemanich, J. Appl. Phys., 91 (2002) 732
[13] H. Ishikawa, S. Kobayashi, Y. Koide, S. Yamasaki, S. Nagai, J. Umezaki, M Koide, J. Appl. Phys., 81 (1997) 1315
[14] F. Peiro, A. Cornet, T.G.G. Maffeus, M.C. Simmonds, and S.A. Clark, Inst. Phys. Conf. Ser., 169 (2001) 463
[15] L.L. Smith, R.F. Davis, M.J. Kim, R.W. Carpenter, and Y. Huang, J. Mater. Res., 12 (1997) 2249
[16] H. S. Venugopalan, S. E. Mohney, B. P. Luther, S. D. Wolter, and J. M. Redwing, J. Appl. Phys., 82 (1997) 650
[17] J.-S. Jang, S.-J. Park, and T.-Y. Seong, J. Electrochem. Soc., 146 (1999) 3425
[18] L.-C. Chen, F.-R. Chen, J.-J. Kai, L. Chang, J.-K. Ho, C.-S. Jong, C. C. Chiu, C.-N. Huang, C.-Y. Chen, and K.-K. Shih, J. Appl. Phys., 86 (1999) 3826
[19] T.G.G. Maffeus, M.C. Simmonds, S.A. Clark, F. Peiro, P. Haines, and P.J. Parbrook, J. Appl. Phys., 92 (2002) 3179
[20] S. W. King, J. P. Barnak, M. D. Bremser, K. M. Tracy, C. Ronning, R. F. Davis, and R. J. Nemanich, J. Appl. Phys., 84 (1998) 5248
[21] J. Dumont, R. Caudano, R. Sporken, E. Monroy, E. Munoz, B. Beaumont, and P. Gibart, MRS Internet J. Nitride Semicond. Res., 5S1 (2000) W11.79
[22] X.A. Cao, E.B. Stokes, P. Sandvik, N. Taskar, J. Kretchmer, and D. Walker, Sol.-State Electronics, 46 (2002) 1235
[23] J.-K. Ho, C.-S. Jong, C.C. Chiu, C.-N. Huang, K.-K. Shih, L.-C. Chen, F.-R. Chen, J.-J. Kai, J. Appl. Phys., 86 (1999) 4491
[24] P.K. Schenck, A.V. Davydov, and D.L. Kaiser, Appl. Surf. Sci., this issue
[25] Y. Hagio, H. Sugahara, T. Maruyama, Y. Nanishi, K. Akimoto, T. Miyajima, and S. Kijima, Jpn. J. Appl. Phys., 41 (2002) 2493
[26] P. Nash (Editor), Phase Diagrams of Binary Nickel Alloys, ASM International, Materials Park, OH, 1991; H. Okamoto and T.B. Massalski (Editors), Phase Diagrams of Binary Gold Alloys, ASM International, Materials Park, OH, 1987

Figure captions

Fig. 1 Au/Ni metallization library deposited on GaN/sapphire. Numbers indicate nominal Ni and Au thicknesses for each metallization element in the array.

Fig. 2 XRD patterns for: **a)** Au(35nm)/Ni (0 nm), **b)** Au(35nm)/Ni(5 nm), **c)** Au(35nm)/Ni(15 nm), **d)** Au(35nm)/Ni(65nm). Angular integrated "Intensity – 2θ" scans (solid white lines) are superimposed on 2-D 2θ-χ GADDS images.
Reflections: 1 – GaN 0002; 2 – Au 111; 3 – Al_2O_3 0006; 4 – Ni 111.

Fig. 3 a) High-resolution TEM image of Au(35 nm)/GaN sample. Au grains are <111> fiber textured with up to 10^o misorientation relative to the surface normal; 2 nm thick amorphous layer (light-gray) is identified between Au and GaN.
b) High-resolution TEM image of Au(35 nm)/Ni(15 nm)/GaN sample near Ni/GaN interface. Two Ni domains, I and II, are related by 60° rotation about [111].
c) Low-resolution TEM image of Au(35 nm)/Ni(15 nm)/GaN sample, illustrating typical morphology: Au grains are an order of magnitude larger than Ni grains.

Fig. 4 EBSD patterns from: **a)** Au(35 nm)/Ni(5 nm); **b)** Au(35 nm)/Ni(65 nm).
Indices with subscripts I and II indicate presence of two Au domains, related by 60° rotation about [111].
Note loss of contrast in pattern (b) due to increased grain misorientation in Au/Ni layers.

Figures:

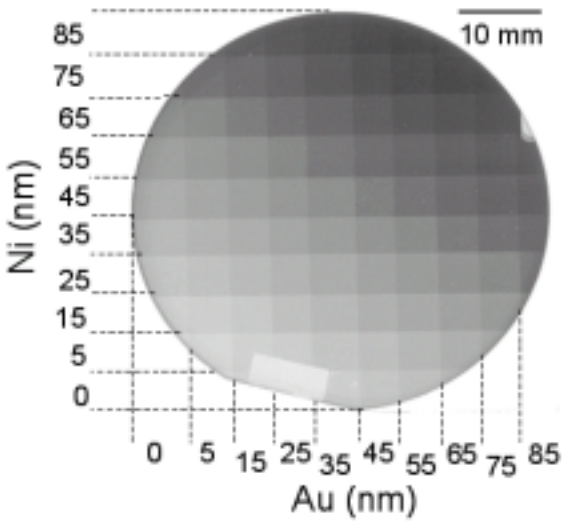

Fig. 1

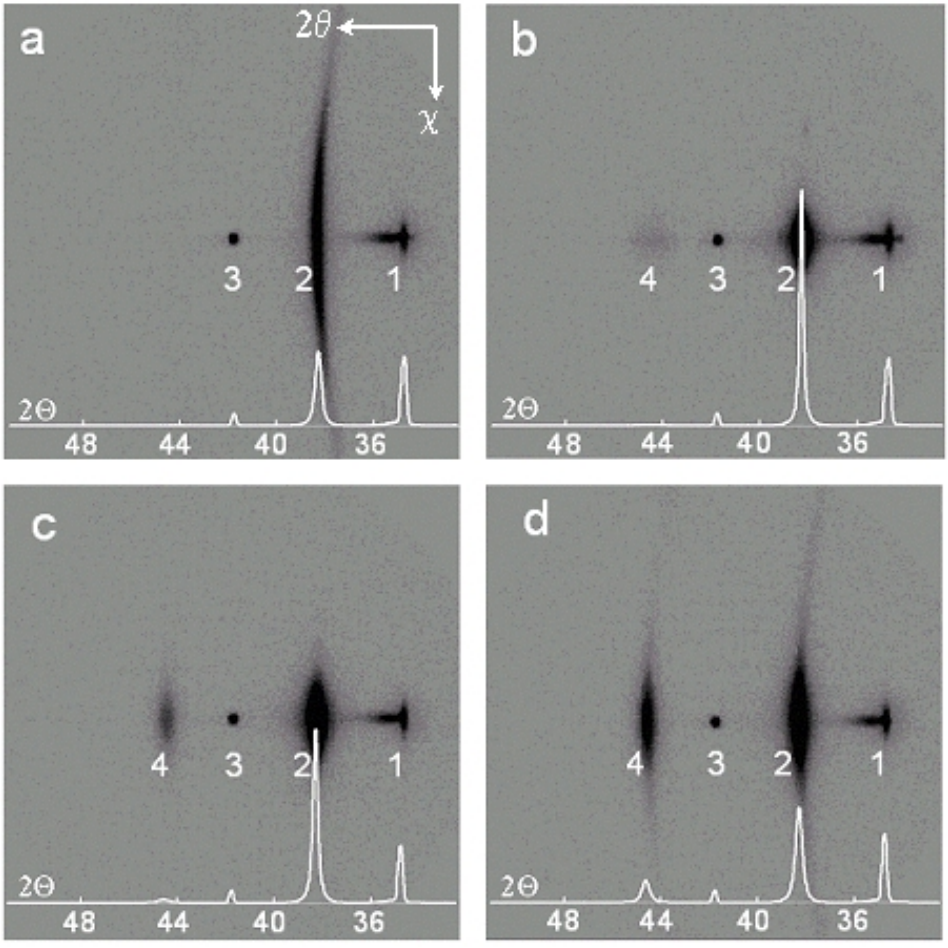

Fig. 2

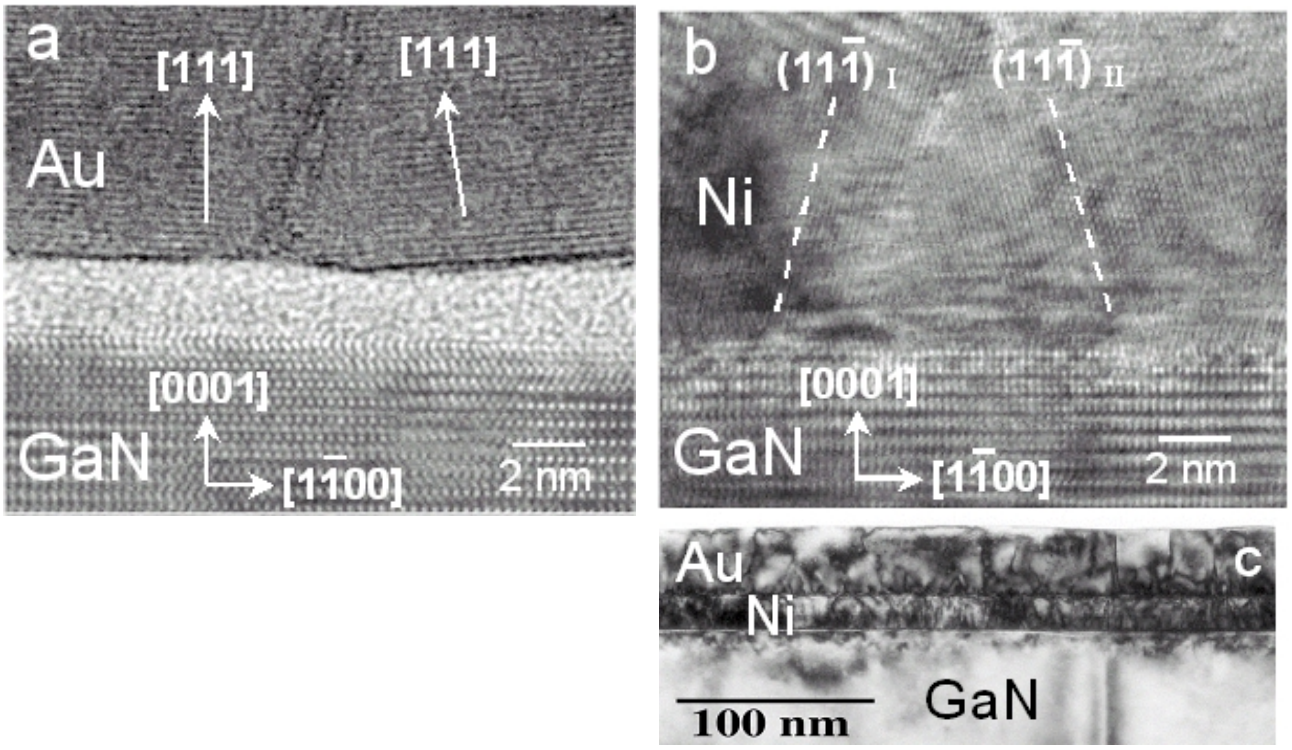
a
[111]
[111]
Au
[0001]
GaN
[1$\bar{1}$00]
2 nm
b
(11$\bar{1}$) I
(11$\bar{1}$) II
Ni
[0001]
GaN
[1$\bar{1}$00]
2 nm
Au
Ni
c
100 nm
GaN

Fig. 3

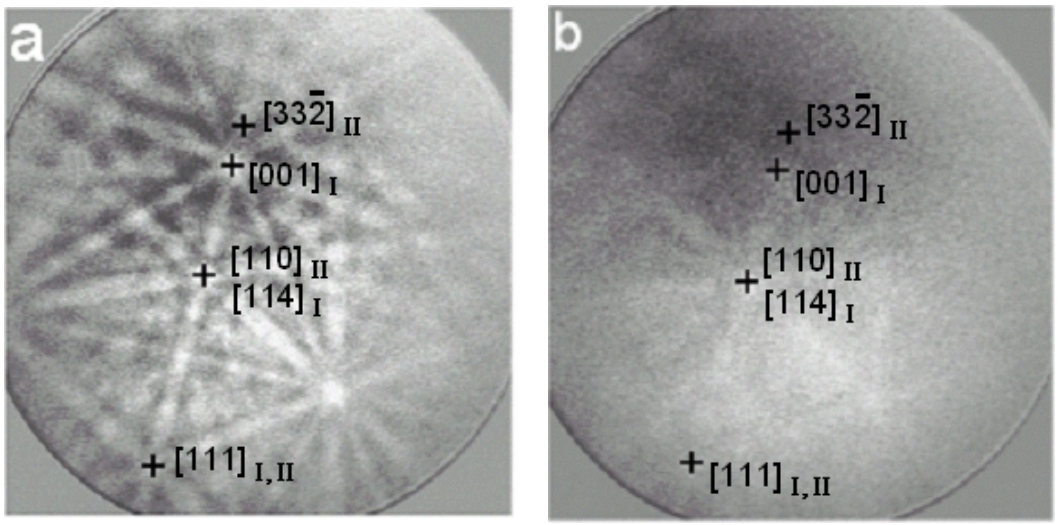
a
+[33$\bar{2}$] II
+[001] I
+[110] II
[114] I
+[111] I,II
b
+[33$\bar{2}$] II
+[001] I
+[110] II
[114] I
+[111] I,II

Fig. 4